Supporting Information

Mechanical Properties of Zeolitic Metal-Organic Frameworks: Mechanically Flexible Topologies and Stabilization against Structural Collapse

T. D. Bennett,*[a] J. Sotelo[b,c], Jin-Chong Tan[d] and S. A. Moggach[b]

[a] *Department of Materials Science and Metallurgy, University of Cambridge, 27 Charles Babbage Road, Cambridge, CB3 0FS United Kingdom.*

Tel: +441223 334342; E-mail: tdb35@cam.ac.uk

[b] *EaStCHEM School of Chemistry, The University of Edinburgh, Kings Buildings, West Mains Road, Edinburgh, EH9 3JJ, United Kingdom.*

[c] *EaStCHEM School of Chemistry, The University of St. Andrews, Purdie Building, North Haugh, St Andrews, Fife, KY16 9ST, United Kingdom.*

[d] Department of Engineering Science, University of Oxford, Parks Road, Oxford OX1 3PJ, UK.

SI-1: Methods

SI-2: Characterization of **1** and **2**

SI-3: Face Indexing

SI-4: Nanoindentation

SI-5: Solvent Accessible Volume Calculations

SI-6: Powder Diffraction and TGA of **1** Containing Ethanol and Butanol

SI-7: Indentation Data for **1** Containing Ethanol

SI-8: Ball Milling

SI-9: Characterization of a_{m}rho-ZMOF

SI-1: Methods

Thermal Gravimetric Analysis (TGA)

TGA was performed on TA Instrument Q500. Typically, 10 mg of sample was placed in an alumina pan under dry N_2 flow (100 mL/min) and heated at a rate of 10 °C/min to 500 °C. Before TGA measurements, all samples were degased thoroughly under vacuum (< 1 mbar) for 5 hours.

Powder X-ray Diffraction

Room temperature PXRD data ($2\theta = 5\text{-}50°$) were collected with a Bruker-AXS D8 diffractometer using Cu $K\alpha_1$ ($\lambda = 1.540598$ Å) radiation and a LynxEye position sensitive detector in Bragg-Brentano parafocusing geometry. Analysis of the data was carried out using the X'pert HighScore Plus program. Structureless pattern profile refinements of low angle data ($2\theta = 5 - 20°$) were also carried out using X'pert HighScore Plus. Refinement of experimental background, cell parameters, W and V parameters and two asymmetry parameters were undertaken, in accordance with previous literature on monitoring the collapse of metal-organic frameworks with applied pressure.[1] The integral breadth of the first diffraction peak at $2\theta \approx 7$ (the last remaining peak upon amorphization) was used instead of the FWHM as the use of an anti-scattering knife-edge on the X-ray diffractometer resulted in an increasing background at low-angle.

Face-Indexing

Face-indexing measurements were performed at room temperature using an Oxford diffraction SuperNova X-ray source using Cu $K\alpha_1$ ($\lambda = 1.540598$ Å) equipped with an Atlas detector. Data were collected in ω-scans in four settings of 2θ and ϕ with a step size of 1°. Exposure time for crystal **1** was 60 s at low angle and 180s at high-angle. For crystal **2** exposure time was 1 s and 40 s at low and high angle respectively. Data processing, unit cell determination and face indexing were carried out using the program CrysAlisPro.

Nanoindentation

Nanoindentation experiments were performed using an MTS Nanoindenter XP, located in an isolation cabinet to shield against thermal fluctuations and acoustic interference.

Single crystals of each sample were first cold-mounted using an epoxy resin and then carefully polished using increasingly fine diamond suspensions. Indentations were conducted under the dynamic displacement-controlled "continuous stiffness measurement" mode. E and H mechanical properties were subsequently determined as a function of the surface penetration depth. A 2-nm sinusoidal displacement at 45 Hz was superimposed onto the system's primary loading signal, and the loading and unloading strain rates were set at 5×10^{-2} s^{-1}. All tests were performed to a maximum indentation depth of 1,000 nm using a Berkovich (i.e., three-sided pyramidal) diamond tip of radius ~ 100 nm. A Poisson's ratio of 0.2 was used, in accordance with prior nanoindentation studies on ZIFs. The raw data (load-displacement curves) obtained were analyzed using the Oliver and Pharr method.[2] Data from depths under 100 nm were not included because of tip -surface contact variance. The effect of anisotropy could not be investigated due to the small size of single crystals of **1**.

Ball Milling

300 mg of the materials were placed inside a 10 mL stainless steel jar alongside a 9 mm stainless steel milling ball at room temperature and sealed properly. This combination was then subjected to 20 Hz milling in a Retsch MM400 grinder mill for 5 minute intervals, after which a sample was taken out, analyzed and replaced.

Microanalysis was performed at the Department of Chemistry, University of Cambridge as a technical service.

FTIR Spectroscopy experiments were performed using a Bruker Tensor 27 Infrared spectrometer.

Extraction of Elastic Modulus of ZIF-8

Matrix inversion performed using Mathcad.

Elastic Constants:

$C_{11} := 9.522$

$C_{12} := 6.865$ GPa

$C_{44} := 0.967$

$$C_{ij} := \begin{pmatrix} C_{11} & C_{12} & C_{12} & 0 & 0 & 0 \\ C_{12} & C_{11} & C_{12} & 0 & 0 & 0 \\ C_{12} & C_{12} & C_{11} & 0 & 0 & 0 \\ 0 & 0 & 0 & C_{44} & 0 & 0 \\ 0 & 0 & 0 & 0 & C_{44} & 0 \\ 0 & 0 & 0 & 0 & 0 & C_{44} \end{pmatrix} = \begin{pmatrix} 9.522 & 6.865 & 6.865 & 0 & 0 & 0 \\ 6.865 & 9.522 & 6.865 & 0 & 0 & 0 \\ 6.865 & 6.865 & 9.522 & 0 & 0 & 0 \\ 0 & 0 & 0 & 0.967 & 0 & 0 \\ 0 & 0 & 0 & 0 & 0.967 & 0 \\ 0 & 0 & 0 & 0 & 0 & 0.967 \end{pmatrix}$$

$$S_{ij} := C_{ij}^{-1} = \begin{pmatrix} 0.2652452 & -0.1111191 & -0.1111191 & 0 & 0 & 0 \\ -0.1111191 & 0.2652452 & -0.1111191 & 0 & 0 & 0 \\ -0.1111191 & -0.1111191 & 0.2652452 & 0 & 0 & 0 \\ 0 & 0 & 0 & 1.0341262 & 0 & 0 \\ 0 & 0 & 0 & 0 & 1.0341262 & 0 \\ 0 & 0 & 0 & 0 & 0 & 1.0341262 \end{pmatrix}$$

Elastic Compliances:

$S_{11} := S_{ij_{1,1}} = 0.265$

$S_{12} := S_{ij_{1,2}} = -0.111$ GPa^{-1}

$S_{44} := S_{ij_{4,4}} = 1.034$

Directional Cosines:

$$L_1(u,v,w) := \frac{u}{\sqrt{u^2+v^2+w^2}} \qquad L_2(u,v,w) := \frac{v}{\sqrt{u^2+v^2+w^2}} \qquad L_3(u,v,w) := \frac{w}{\sqrt{u^2+v^2+w^2}}$$

Cubic System:

$u := -1 \quad v := -1 \quad w := 2$

$L1 := L_1(u,v,w) \qquad L2 := L_2(u,v,w) \qquad L3 := L_3(u,v,w)$

$$S_{uvw} := S_{11} - 2\left(S_{11} - S_{12} - \frac{1}{2}S_{44}\right)\cdot\left(L1^2\,L2^2 + L2^2\,L3^2 + L3^2\,L1^2\right) = 0.336$$

$$E_{uvw} := \frac{1}{S_{uvw}} = 2.9798$$ GPa

E(100) = 3.77 GPa

E(110) = 2.98

E(111) = 2.79

E(-1 -1 2) = E(112) = 2.98

SI-2: Powder X-ray Diffraction and TGA of **1** and **2**

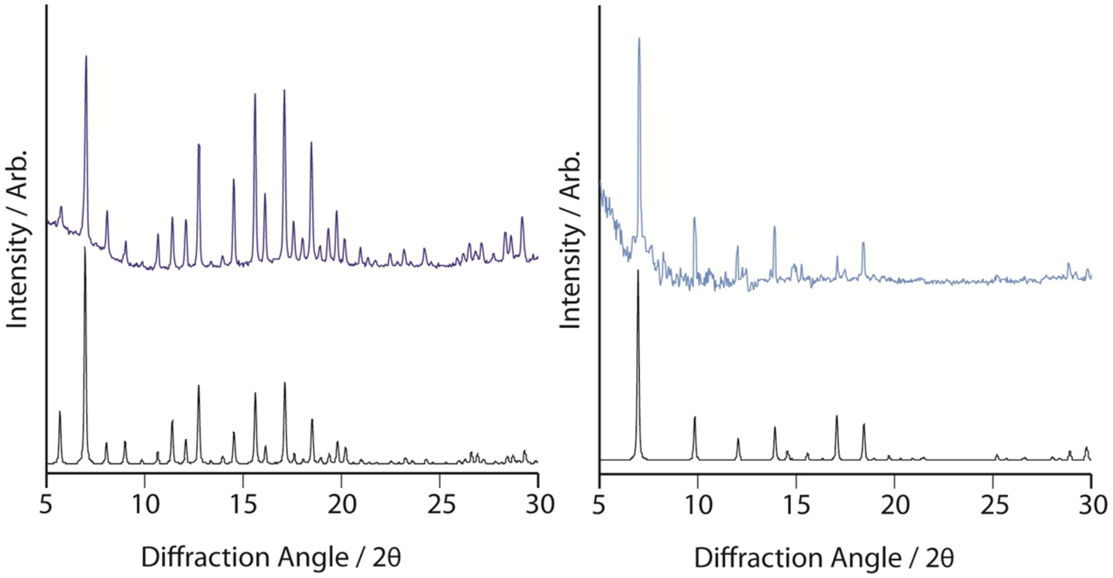

Figure S1: Powder X-ray diffraction patterns of (left) evacuated rho-ZMOF and (right) evacuated sod-ZMOF, along with simulated diffraction patterns. The latter was unable to be obtained in a completely phase pure manner.

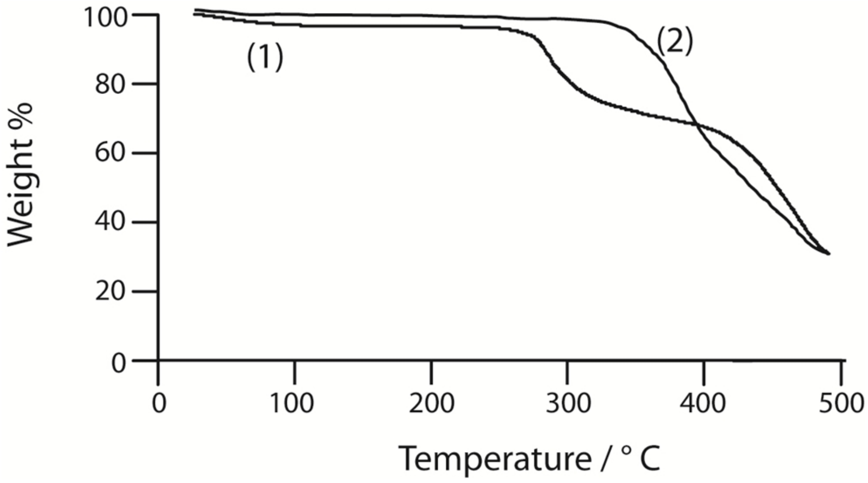

Figure S2: Thermogravimetric analysis of **1** and **2** confirming evacuation.

SI-3: Face Indexing

Rho-ZMOF face-indexing experimental details:

Crystal system	Cubic	
Space group	*Im*-3*m*	
Unit cell dimensions	a = 30.990(6) Å	α=90°
	b = 30.990(6) Å	β=90°
	c = 30.990(6) Å	γ=90°
Volume	29762(10) $Å^3$	
Crystal size	0.125 x 0.139 x 0.142 mm	
Measured reflections used	1083	

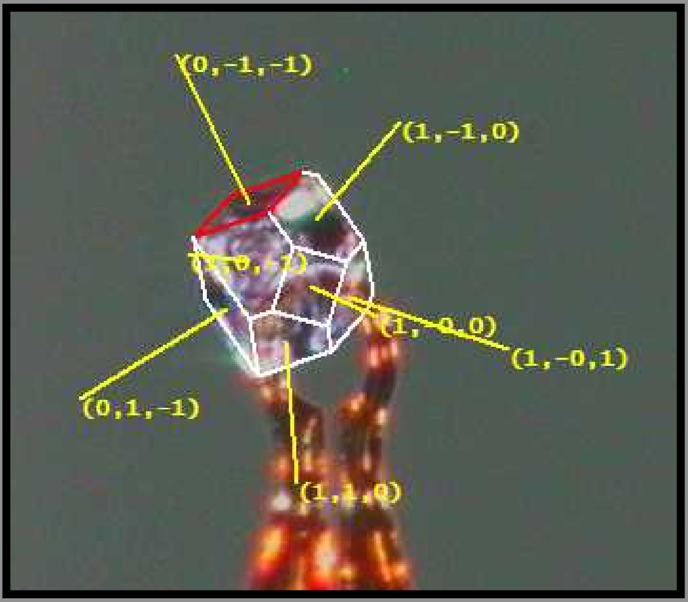

Figure S3: Face indexing of **1**.

Sod-ZMOF face-indexing experimental details:

Crystal system	Cubic	
Space group	*Fd*-3*c*	
Unit cell dimensions	a = 35.9314(7) Å	α=90°
	b = 35.9314(7) Å	β=90°
	c = 35.9314(7) Å	γ=90°
Volume	46390(3) $Å^3$	
Crystal size	0.2954 x 0.2723 x 0.1584 mm	
Measured reflections used	4339	

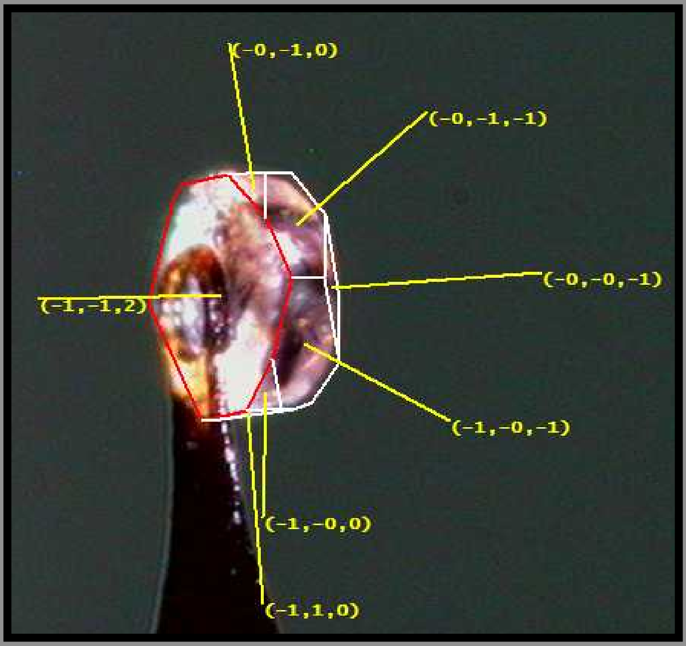

Figure S4: Face indexing of **2**.

SI-4: Nanoindentation

25 indents were performed overall across two crystals of **1**. Load-displacement data were consistent across all of the indents. An equal number of indents were performed on two crystals of **2**, though the facet enabled a larger spacing to be left between indents. It is noted that since measurements of H by nanoindentation depend strongly upon experimental set up and tip calibration, it is generally only possible to accurately compare values with other MOFs indented using an identical experimental set up.

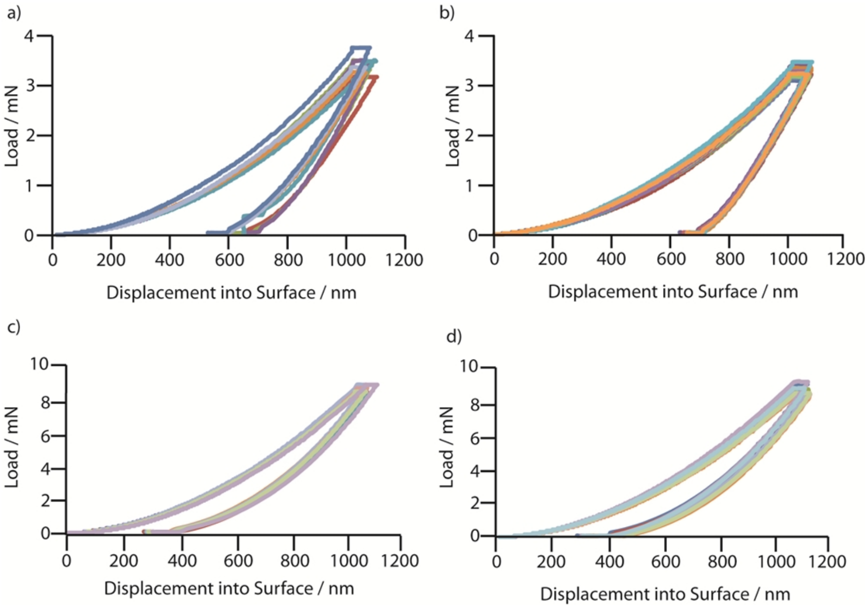

Figure S5: Load vs indentation curves for the two crystals of **1** (a and b) and **2** (c and d) indented.

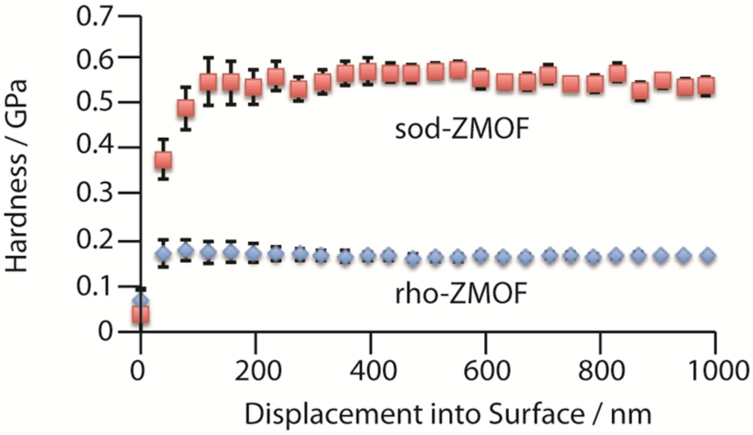

Figure S6: Hardness values as a function of depth for **1** and **2**.

SI-5: Solvent Accessible Volume Calculations

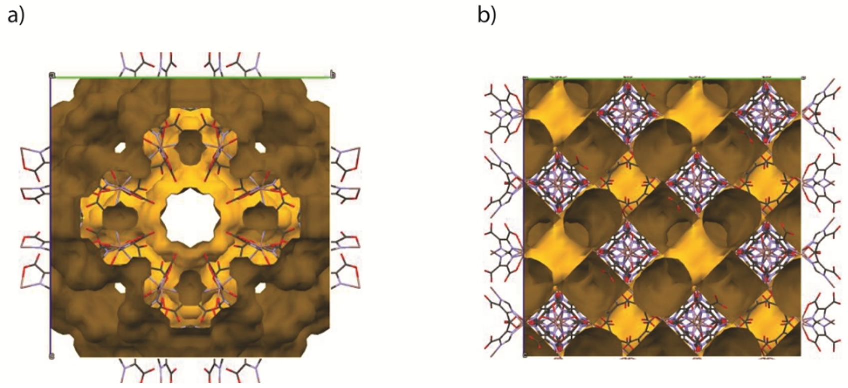

Figure S7: Solvent accessible volumes of **1** and **2**. Void Analysis was carried out using a probe radius of 1.2 Å and grid spacing of 1.0 Å, using the program Mercury.[3]

SI-6: Powder Diffraction and TGA of **1** Containing Ethanol and Butanol

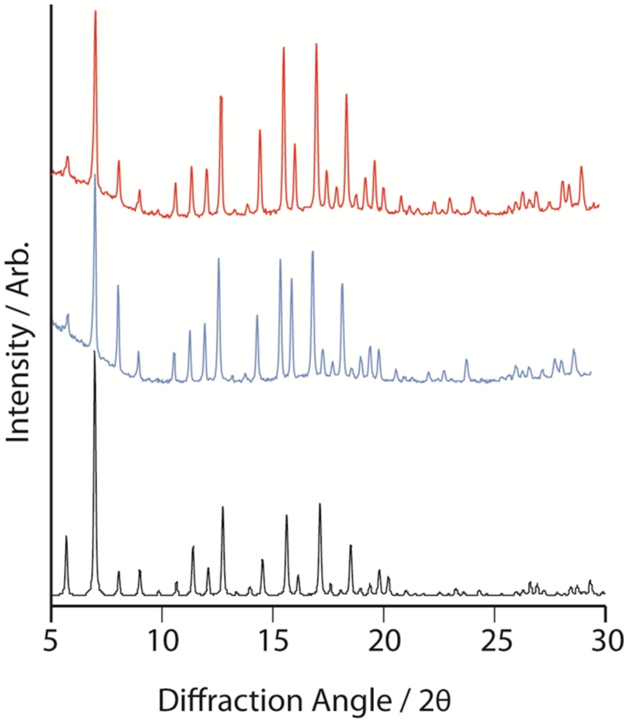

Figure S8: Powder X-ray diffraction patterns of rho-ZMOF. Calculated (bottom), after soaking in ethanol (middle) and after soaking in butanol (top). Structural integrity is retained in all cases.

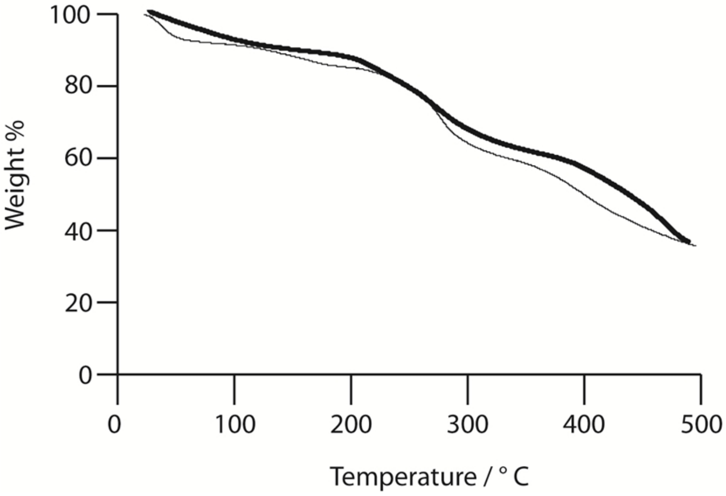

Figure S9: Thermogravimetric analysis of **1** after soaking in ethanol (thin trace) and butanol (thick trace). Weight losses at 200 °C suggest adsorption of 13.71 % ethanol and 11.11 % butanol respectively.

SI-7: Indentation Data for **1** containing ethanol

A single crystal of **1** exposed to ethanol was indented 20 times in total, and the data compared to the two evacuated samples already indented.

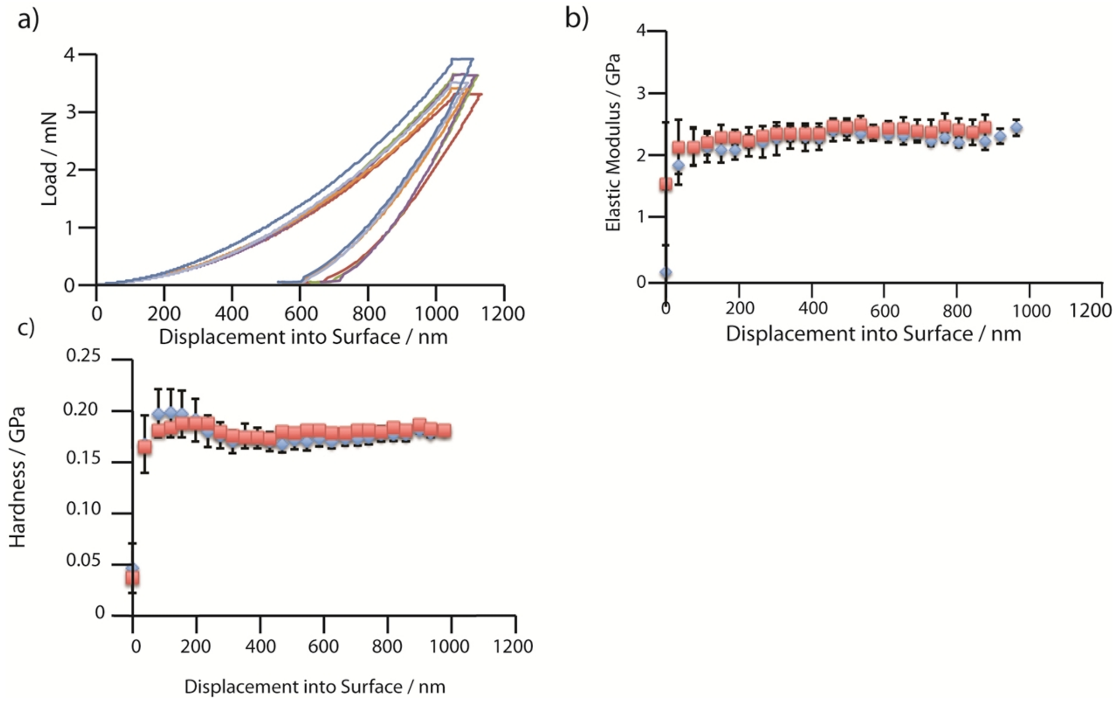

Figure S10: (a) Load –displacement, (b) elastic modulus – displacement and (c) hardness – displacement data for a single crystal of **1** exposed to ethanol. Error bars represent standard deviations from more than 15 tests. Red – representative data for the solvent containing sample, blue –representative data for the evacuated sample.

SI-8: Ball-Milling

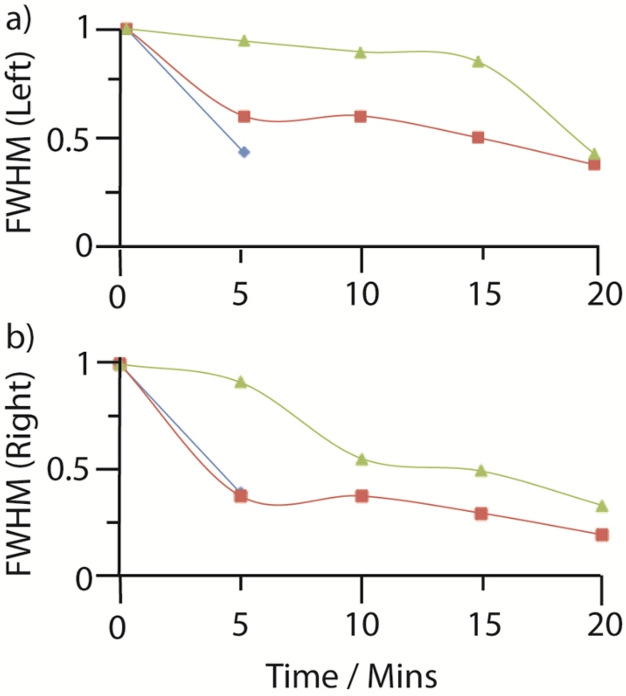

Figure S11: Evolution of the full width at half maximum of the diffraction peak at 2θ ≈ 7 for bulk samples of **1** evacuated (blue), containing ethanol (red) and butanol (green).

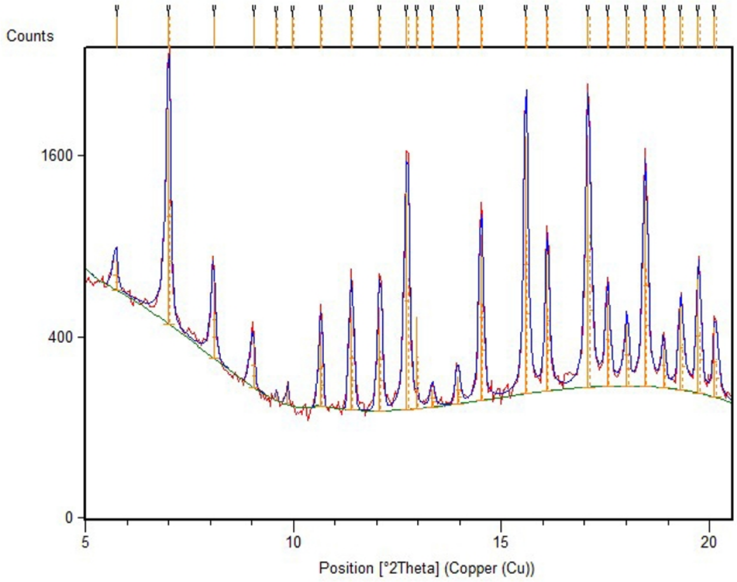

Figure S12: Structureless pattern profile refinement plot of **1**.

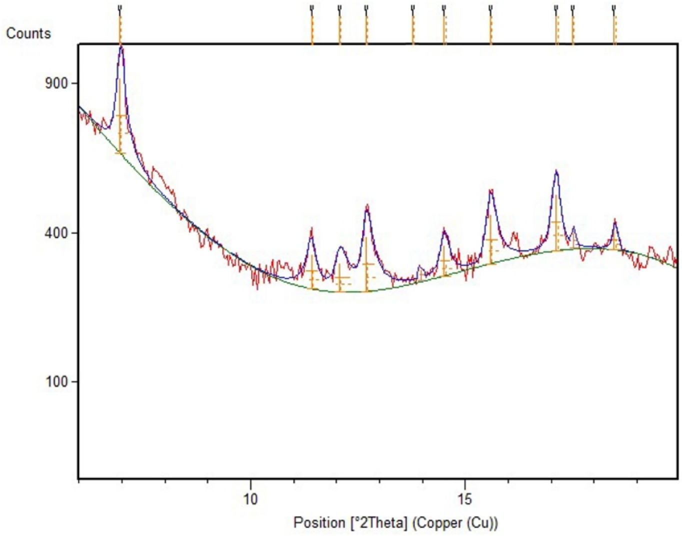

Figure S13: Structureless pattern profile refinement plot of **1** after ball-milling for 5 minutes.

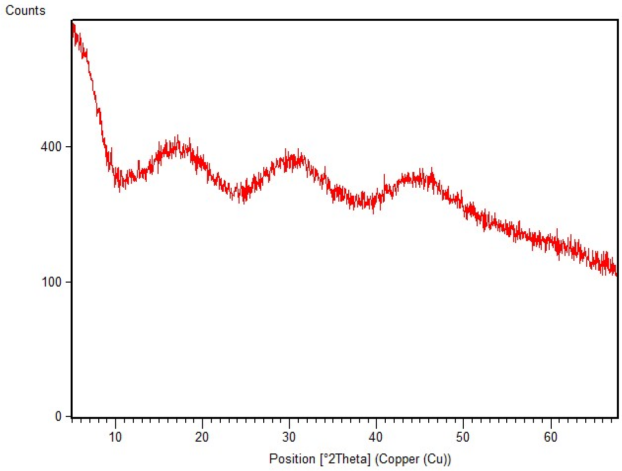

Figure S14: Powder X-ray diffraction pattern of **1** after ball-milling for 10 minutes.

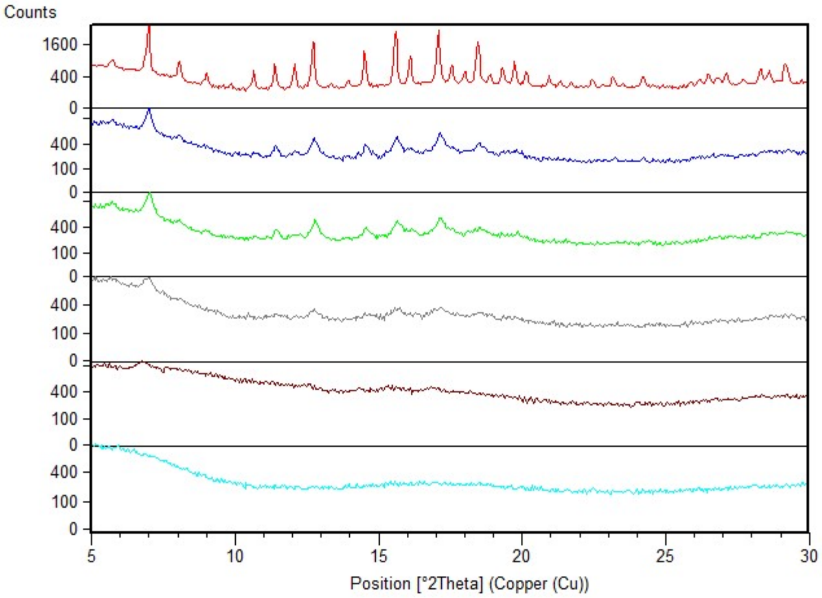

Figure S15: Powder X-ray diffraction patterns of **1** containing ethanol with increasing milling times.

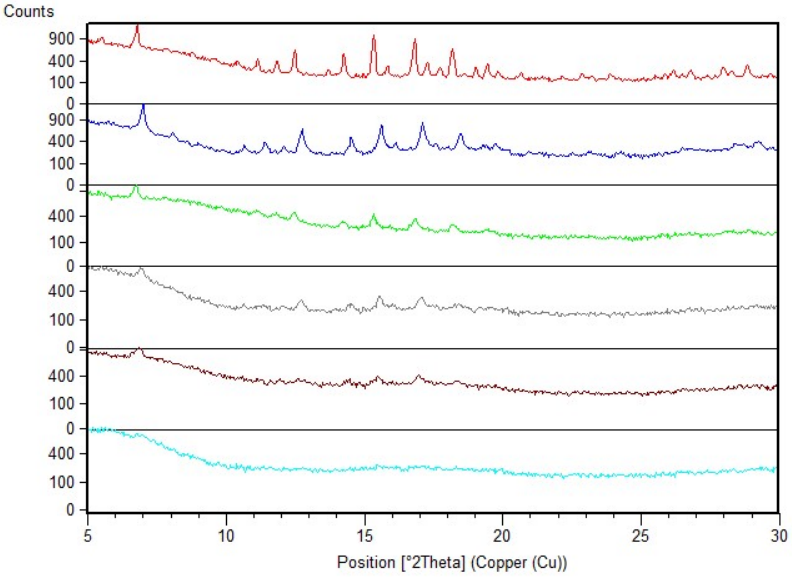

Figure S16: Powder X-ray diffraction patterns of **1** containing butanol with increasing milling times.

SI-9: Characterization of Ball-Milling Products

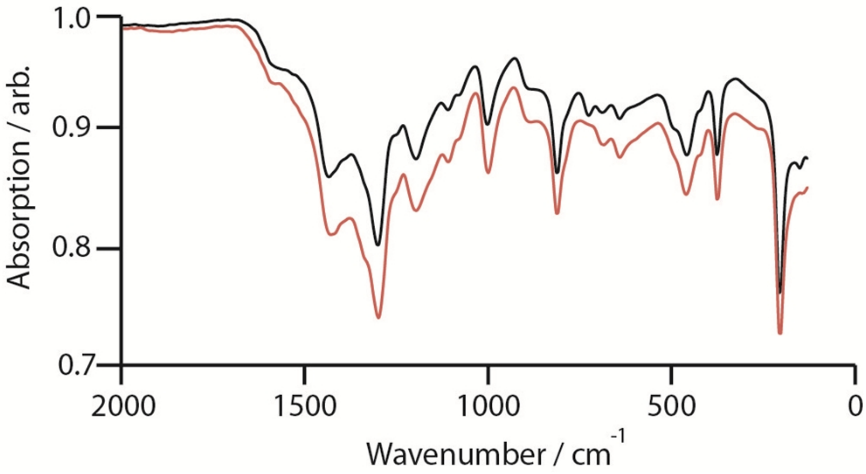

Figure S17: Low wavenumber region of the FTIR spectra for evacuated rho-ZMOF (red) and ball-milled rho-ZMOF (black).

Elemental analysis of evacuated (crystalline) rho-ZMOF:

Calculated (based on [DMA·In(HImDC)$_2$]: C 30.7 %, H 2.56 %, N 14.93 %

Found : C 29.41 %, H 1.91 %, N 15.56 %

and ball-milled (amorphous) rho-ZMOF:

Calculated (based on [DMA·In(HImDC)$_2$]: C 30.7 %, H 2.56 %, N 14.93 %

Found : C 30.23 %, H 1.82 %, N 15.98 %

References

1. V. Guillerm, F. Ragon, M. Dan-Hardi, T. Devic, M. Vishnuvarthan, B. Campo, A. Vimont, G. Clet, Q. Yang, G. Maurin, G. Férey, A. Vittadini, S. Gross and C. Serre, *Angew. Chem. Int. Ed.*, 2012, **51**, 9267-9271.
2. W. C. Oliver and G. M. Pharr, *J Mater Res*, 2004, **19**, 3-20.
3. C. F. Macrae, I. J. Bruno, J. A. Chisholm, P. R. Edgington, P. McCabe, E. Pidcock, L. Rodriguez-Monge, R. Taylor, J. van de Streek and P. A. Wood, *J Appl Crystallogr*, 2008, **41**, 466-470.